Vol 18 No 2, February 2009
1674-1056/2009/18(02)/0630-06

Chinese Physics B

© 2009 Chin. Phys. Soc.
and IOP Publishing Ltd

Effect of interstitial air holes on Bragg gratings in photonic crystal fibre with a Ge-doped core*

Zhang Hui-Jia(张慧嘉), Li Shu-Guang(李曙光)†, and Hou Lan-Tian(侯蓝田)

State Key Laboratory of Metastable Materials Science and Technology, College of Science, Yanshan University, Qinhuangdao 066004, *China*

(Received 23 August 2007; revised manuscript received 11 July 2008)

The effect of interstitial air holes on Bragg gratings in photonic crystal fibre (PCF) with a Ge-doped core is numerically investigated by using the beam propagation method (BPM). It is shown that the interstitial air holes (IAHs) can make Bragg resonance wavelength λ_B shift a little towards short wavelengths and increase $\lambda_B - \lambda_1$ (the wavelength spacing between the main peak with Bragg resonance wavelength λ_B and the first side peak with wavelength λ_1) and the coupling coefficient κ of Bragg resonance. Moreover, when the ratio of air hole diameter (d) to pitch (Λ), d/Λ, is small, IAHs can suppress the cladding mode resonance. When d/Λ is large, IAHs increase the number of mode that could strongly interact with the fundamental mode. By comparing the transmission spectral characteristics of PCF-based fibre Bragg grating (FBG) with IAHs with those without IAHs at the same air-filling fraction, it is clarified that the change of transmission spectral characteristics of PCF-based FBG with IAHs is not due to a simple change in air-filling fraction. It is also closely related to the distribution of interstitial air holes.

Keywords: photonic crystal fibre, fibre grating, beam propagation method, interstitial air holes
PACC: 4281, 4280S, 4280F

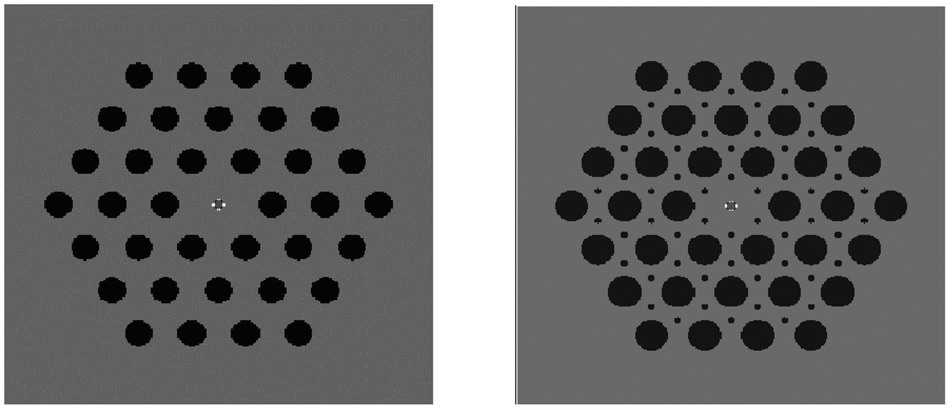
1. Introduction

Since Knight *et al*[1] fabricated the first photonic crystal fibre (PCF) in 1996, PCF has attracted many researchers' attention. Because the PCF has various unique features and can be designed flexibly,[2,3] its emergence makes the fibre Bragg grating (FBG) enter into a new research area.[4] Compared with conventional FBG, PCF-based FBG has some unique features.[4,5]

The interstitial air holes (IAHs) are located at a midpoint between three holes in triangular lattice and are caused by the stack and draw fabrication technique used for fabricating PCFs.[1] Broeng *et al*[6] have proposed a photonic bandgap (PBG) structure with interstitial holes in order to increase the bandgap size. Li *et al*[7] have studied honeycomb photonic bandgap fibres (HPBFs) with and without interstitial air holes separately. Li *et al*[8] and Yu *et al*[9] have studied the basic properties of index-guiding photonic crystal fibres (IGPCFs) with and without IAHs, separately. Kim *et al*[10] have investigated the spectral properties of a long-period fibre grating written in photonic crystal fibre that has interstitial air holes. It was found that the interstitial air holes of the photonic crystal fibre played a critical role in restricting the number of modes that could strongly interact with the fundamental mode and in obtaining well-separated resonance peaks. The work was motivated by the interest in the influence of small interstitial air holes which remained in the fibre cladding after drawing on Bragg gratings in photonic crystal fibres with a Ge-doped core. Cross sections of PCFs with and without IAHs are schematically shown in Fig.1(a) and Fig.1(b), respectively. The grey regions are silica, while the black regions are air. A Ge-doped core is situated in the centre of PCF's cross sections.

In this paper, we numerically study the basic properties of PCF-FBG with and without IAHs by using the beam propagation method (BPM).[11,12] The BPM method provides a simple intuitive method of determining the modal spectrum and modal profiles for a waveguide. It has been used extensively in the study of complex waveguides, and it is well suited to computing mode evolution in waveguides that vary in the longitudinal direction and in the geometry where leaky modes are important. This latter point is of particular interest in this work where we consider the

*Project supported by the National Natural Science Foundation of China (Grant No 10874145), and the Yanshan University Doctoral Foundation (Grant No B153).
†E-mail: shuguangli@ysu.edu.cn



(a) (b)

Fig.1. Cross sections of PCFs without (a) and with IAHs (b). The grey regions are silica, while the black regions are air. A Ge-doped core is situated in the centre of PCF's cross sections.

propagation of leaky cladding modes in different air-silica fibres. In this simulation, we assume that the grating does not strongly affect the modal properties of the guide, and so we can model PCF corresponding to the grating for solving mode.[11,13] For wavelengths close to the Bragg resonance we can ignore the wavelength dependence of n_{core} and n_{clad} where n_{core} is the effective refractive index of the fundamental mode and n_{clad} is the effective refractive index of the fundamental space-filling mode.

It is shown that the IAHs can reduce Bragg resonance wavelength λ_{B} and increase the wavelength spacing $\lambda_{\mathrm{B}}-\lambda_1$ between the main peak with Bragg resonant wavelength λ_{B} (due to core mode) and the first side peak with wavelength λ_1 (due to the first-order cladding mode), and simultaneously increase coupling coefficient κ of Bragg resonance. Moreover, when ratio of air hole diameter (d) to pitch (Λ), d/Λ, is small, the IAHs can suppress the cladding mode resonance. When d/Λ is large, the IAHs can increase the number of modes that could strongly interact with the fundamental mode.

2. Numerical results and discussion

In the numerical simulation, we consider a PCF with a triangular lattice of air hole as shown in Fig.1. The data used in our simulation are as follows: the lattice pitch (Λ) is $10\,\mu$m, i.e. $\Lambda = 10\,\mu$m; the values of ratio (d/Λ) of air hole diameter (d) to pitch (Λ) are 0.5, 0.6, 0.7 and 0.8 separately, while the values of diameters of IAHs (p_1, p_2 and p_3) are 0.5, 1 and $1.5\,\mu$m respectively, i.e. $p_1 = 0.5\,\mu$m, $p_2 = 1\,\mu$m and $p_3 = 1.5\,\mu$m; the length of PCF is 1 cm; the refractive index of silica is 1.44402; the fibre has a Ge-doped core with diameter $D_{\mathrm{core}} = 2\,\mu$m; the relative difference in refractive index difference between the Ge-doped core and pure silica is 0.3%. The Bragg grating is fabricated on the Ge-doped core with period $\Lambda_{\mathrm{FBG}} = 0.5375\,\mu$m and the grating refractive index modulation $\Delta n = 4.0 \times 10^{-5}$. To clarify whether the change of the transmission spectral characteristics in the presence of interstitial holes arises simply from the change in air-filling fraction, we compare the transmission spectral characteristics of PCF-based FBG without IAHs at the same air-filling fraction with those of the PCF-based FBG with IAHs $p_2 = 1\,\mu$m. Accordingly, the values of ratio d/Λ are 0.520, 0.616, 0.714 and 0.812 separately. A correlation mode solver[12] is used to derive the effective index of the excited mode and the power fraction α^2 in the input field contained in excited mode. The resonant wavelengths corresponding to these modes are calculated from expressions (1) and (2). Coupling coefficient κ of Bragg resonance is calculated from expression (7). The parameters used in BPM are as follows: the initial launched profile is a symmetric Gaussian beam centred on axis of the core, whose width is $2\,\mu$m the same as the core diameter; the longitudinal propagation distance is 1 cm; the number of grid points along the longitudinal direction is 1340; the number of grid points along the transversal direction is 320 with transparent boundary condition. We validate the simulation tool by comparing our simulation results with those by Eggleton *et al.*[4] We analyse a Ge-doped core photonic crystal fibre with a hexagonal array of holes.

For fundamental and higher order guided modes, $n_{\rm eff}$ values derived from our BPM modelling are in good agreement with those measured by Eggleton *et al*:[4] their difference is only below 4×10^{-4}.

Figure 2 shows the influence of IAH diameter P on Bragg resonant wavelength $\lambda_{\rm B}$. In the PCF-based FBG, the Bragg resonant wavelength of the fundamental mode can be determined by using the Bragg condition

$$\lambda_{\rm B} = 2n_{\rm core}\Lambda_{\rm FBG}, \tag{1}$$

where $\Lambda_{\rm FBG}$ is the period of the FBG, and $n_{\rm core}$ is the effective refractive index of the fundamental mode.

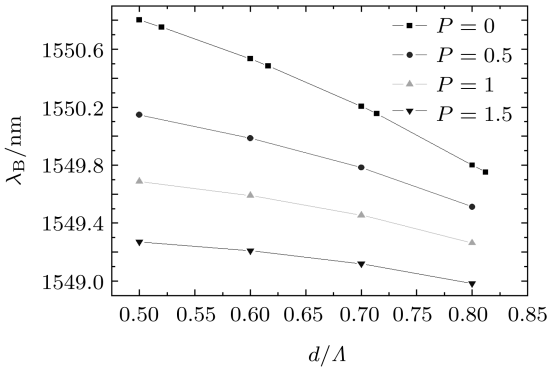


Fig.2. Effect of the IAH diameter P on Bragg resonant wavelength $\lambda_{\rm B}$.

The curve for $P = 0\,\mu$m represents the results of PCFs without IAHs, while the other curves for $P = 0.5$, 1, and $1.5\,\mu$m describe the results of PCFs with IAHs, where P denotes the IAH diameter. There are four points corresponding to $d/\Lambda = 0.520$, 0.616, 0.714, and 0.812 separately on the curve for P=0 μm. These four points have the same air-filling fractions as those for four points $d/\Lambda = 0.5$, 0.6, 0.7, 0.8, respectively in the curve for $P = 1\,\mu$m. Figures 3 and 4 have four points similar to those in Fig.2, respectively.

From Fig.2 we can find the following points: (i) IAHs could make the Bragg resonant wavelength $\lambda_{\rm B}$ shift a little towards short wavelengths. Moreover, the larger the diameter P of IAH is, the shorter the Bragg resonant wavelength $\lambda_{\rm B}$ will be; (ii) at the same air-filling fraction, the Bragg resonant wavelength $\lambda_{\rm B}$ of PCF-based FBG with IAHs is considerably shorter than that without IAHs; (iii) the increase of the value d/Λ leads to a smaller $\lambda_{\rm B}$ in the same curve; (iv) comparing the two curves with IAHs and without IAHs shows that the increase of the value d/Λ makes $\lambda_{\rm B}$ of PCF-based FBG with IAHs shift less towards short wavelengths.

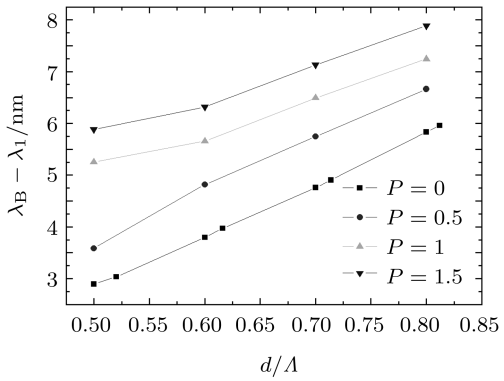


Fig.3. Effect of IAHs diameter P on wavelength spacing $\lambda_{\rm B} - \lambda_1$.

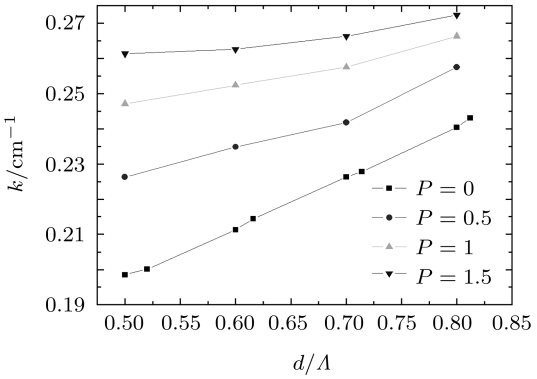


Fig.4. Effect of the IAH diameter P on coupling coefficient κ.

Figure 3 shows the effect of the IAH diameter P on wavelength spacing $\lambda_{\rm B} - \lambda_1$. The resonance wavelength of the cladding modes can be determined by using the phase-matching condition for a cladding resonance[14] to be

$$\lambda_i = (n_{\rm core} + n_{{\rm clad},i})\Lambda_{\rm FBG}, \tag{2}$$

where $n_{{\rm clad},i}$ is the effective refractive index of the i-th cladding mode propagating in the direction opposite to that of the fundamental mode. The wavelength spacing $\lambda_{\rm B} - \lambda_1$ between the main peak with Bragg resonant wavelength $\lambda_{\rm B}$ (due to core mode) and side peak with wavelength λ_1 (due to the first-order cladding mode) is expressed as

$$\lambda_{\rm B} - \lambda_1 = (n_{\rm core} - n_{{\rm clad},1})\Lambda_{\rm FBG}. \tag{3}$$

Figure 3 reveals the following points: (i) wavelength spacing $\lambda_{\rm B} - \lambda_1$ increases due to the presence of IAHs. Moreover, the larger the diameter P of IAH is, the larger the wavelength spacing $\lambda_{\rm B} - \lambda_1$ will be; (ii) at the same air-filling fraction, $\lambda_{\rm B} - \lambda_1$ of PCF-based FBG with IAHs is considerably larger than that

without IAHs; (iii) on the same curve, the increase of the value d/Λ leads to a larger $\lambda_B - \lambda_1$.

Figure 4 shows the effect of the IAH diameter P on coupling coefficient κ of Bragg resonance.

The initial launched profile is

$$E(x, y, 0) = \Delta n(x, y) E_{\text{core}}(x, y). \tag{4}$$

The strength α_i in the launched profile is identical to the coupling coefficient k for coupled mode analysis:[13]

$$\begin{aligned} \alpha_i &= (\lambda/\pi)\kappa_i \\ &= \int_\Omega E_i^*(x, y) E_{\text{core}}(x, y) \Delta n(x, y) \mathrm{d}x\mathrm{d}y. \end{aligned} \tag{5}$$

When the initial launched profile is

$$E(x, y, z) = E_{\text{core}}(x, y), \tag{6}$$

expression (5) is transformed into

$$\begin{aligned} \Delta n(x, y) \int_\Omega E_i^*(x, y) E_{\text{core}}(x, y) \mathrm{d}x\mathrm{d}y &= \Delta n(x, y)\alpha_i \\ &= (\lambda/\pi)\kappa_i \end{aligned}$$

$$k_i = (\pi \Delta n/\lambda)\alpha_i, \tag{7}$$

where $\Delta n(x, y)$ is the grating refractive index modulation, $E_{\text{core}}(x, y)$ is the electric field of the fundamental mode, and $E^*_{\text{core}}(x, y)$ is the electric field of core mode in the direction opposite to that of fundamental mode, Ω denotes the region of grating, and α_i is the amplitude strength of the ith mode.

From Fig.4 we can see that (i) coupling coefficient κ of Bragg resonance increases due to the presence of IAHs. Moreover, the larger the diameter P of IAH, the larger the coupling coefficient κ; (ii) at the same air-filling fraction, coupling coefficient κ of Bragg resonance of PCF-based FBG with IAHs is considerably larger than that without IAHs; (iii) the increase of the value d/Λ leads to a larger coupling coefficient κ in the same curve; (iv) comparing the two curves with IAHs and without IAHs, the increase of the value d/Λ makes coupling coefficient κ of Bragg resonance of PCF-based FBG with IAHs increase less.

Those results can be explained qualitatively as follows: according to the effective index model, n_{clad} is the effective index of the fundamental space-filling mode. n_{core} is the effective index of fundamental mode. The presence of IAHs can reduce the values of n_{core} and n_{clad}, but its effect on n_{clad} is more significant than that on n_{core}.[9] So $n_{\text{core}} - n_{\text{clad}}$ is larger. Accordingly λ_B and $\lambda_B - \lambda_1$, given respectively in expressions (1) and (3), reduce. Because the value of $n_{\text{core}} - n_{\text{clad}}$ is larger, light confined to the fibre core is more, coupling coefficient κ of Bragg resonance is larger according to expressions (5) and (7).

We investigate the effect of interstitial air holes on cladding resonance in FBG-PCF, also (IAHs diameter $P = 1\,\mu$m). We calculate the mode spectrum from $d/\Lambda = 0.2$ to 0.8. Computed mode spectra[15,16] are as follows: the vertical axis represents the relative power fraction α^2 in the input field contained in that mode, and it is proportional to the square of the coupling coefficient k as shown in expression (7). Horizontal axis represents the difference in $n_{\text{eff}} - n_{\text{bar}}$ between the modes without and with IAHs ($n_{\text{bar}} = 1.44402$).

From Fig.5 to Fig.8, we can see that generally, the presence of IAHs strengthens the first cladding mode resonance. When d/Λ is small, IAHs suppress the other cladding mode resonance. When d/Λ is large, IAHs increase the number of modes that could strongly interact with the fundamental mode.

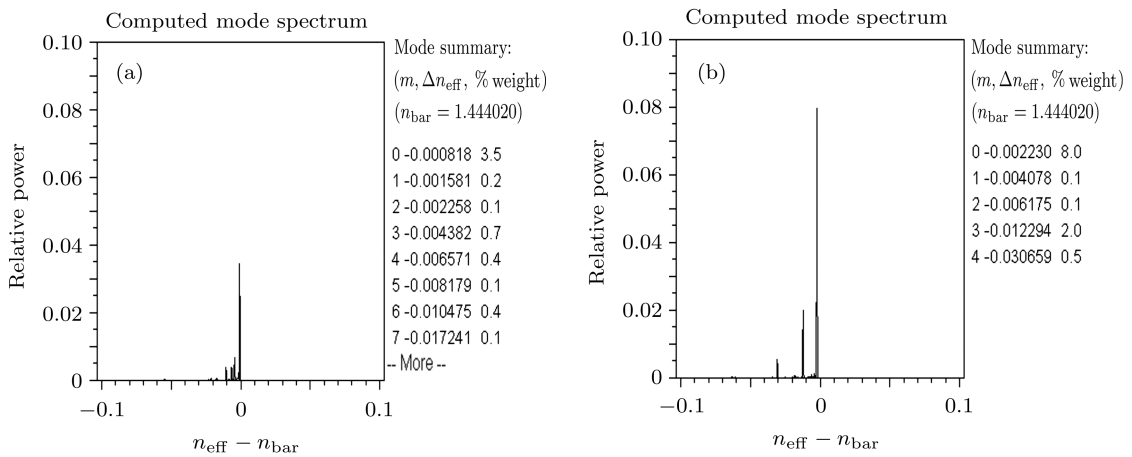


Fig.5. Relative power versus the difference in $n_{\text{eff}} - n_{\text{bar}}$ for $d/\Lambda = 0.2$ without IAHs (a) and with IAHs (b).

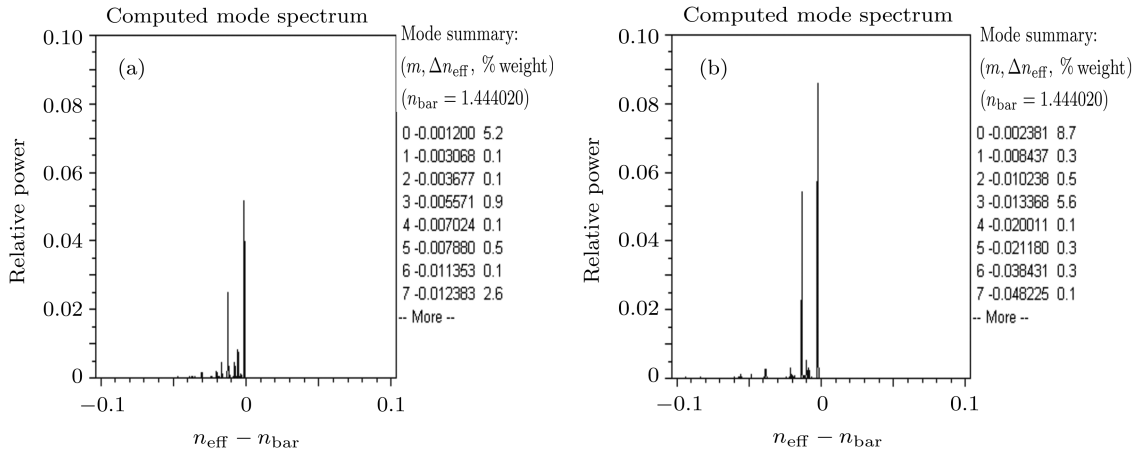


Fig.6. Relative power versus the difference in $n_{\rm eff} - n_{\rm bar}$ for $d/\Lambda = 0.4$ without IAHs (a) and with IAHs (b).

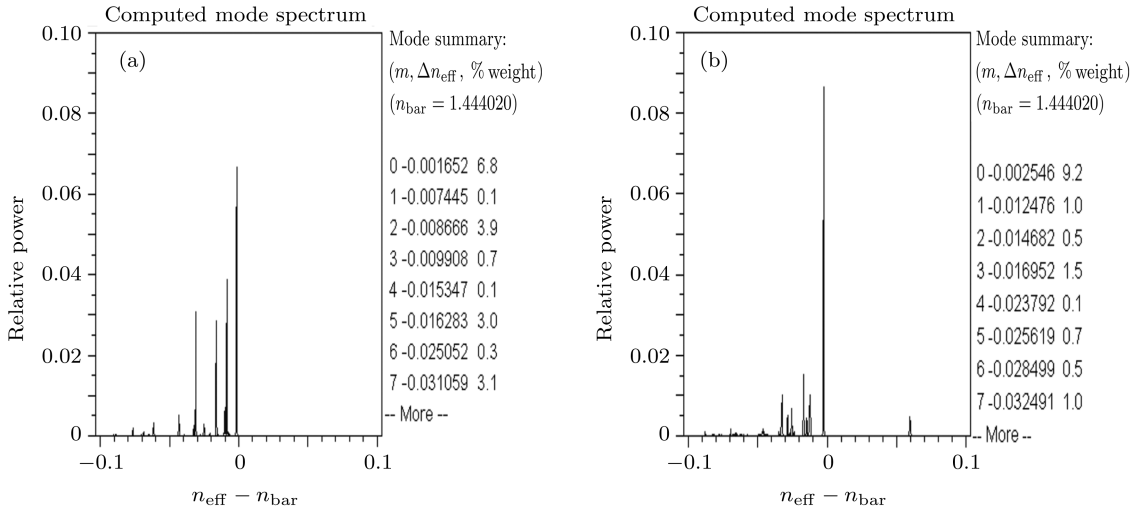


Fig.7. Relative power versus the difference in $n_{\rm eff} - n_{\rm bar}$ for $d/\Lambda = 0.6$ without IAHs (a) and with IAHs (b).

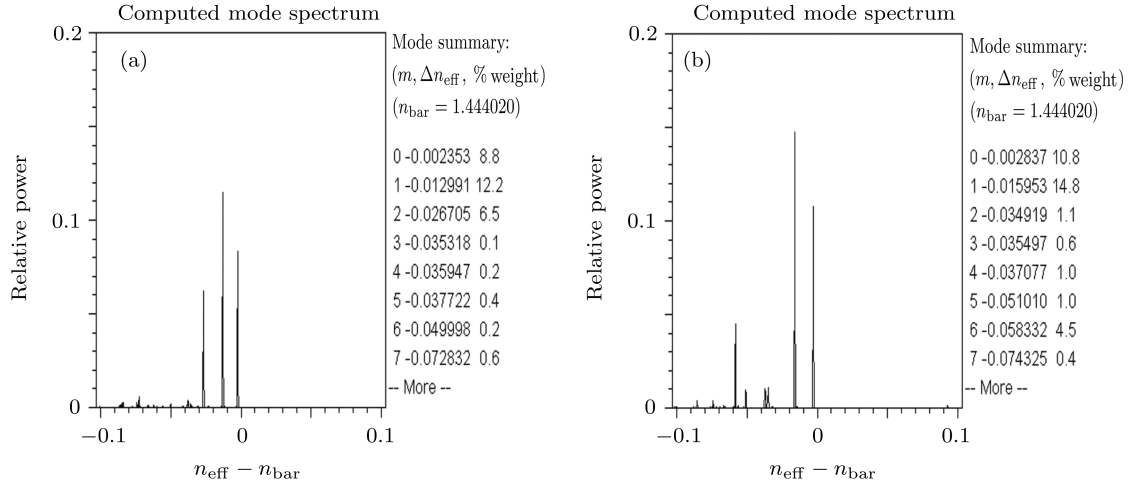


Fig.8. Relative power versus the difference in $n_{\rm eff} - n_{\rm bar}$ for $d/\Lambda = 0.8$ without IAHs (a) and with IAHs (b).

We believe that the presence of IAHs (especially the presence of the most inner layer IAHs) can reduce the effective inner cladding diameter to suppress the most cladding mode resonance.[10,11] But on the other hand, the presence of IAHs increases the confinement effect to increase the number of modes that could

strongly interact with the fundamental mode. Because IAHs are located at a midpoint between three holes in a triangular lattice, we can observe from the geometry structure of PCF-FBG that when d/Λ is very large, the presence of IAHs does not obviously reduce the effective inner cladding diameter. Moreover, PCF becomes a multi-mode fibre in the case. Most of cladding modes are confined in the inner cladding. So in the case, the dominant effect of IAHs is confinement effect to promote the cladding resonance. For the same reason, when the value of d/Λ is small, the dominant effect of IAHs reduces the effective inner cladding diameter to suppress the resonance of the most cladding modes.

3. Conclusions

We have numerically investigated the effect of interstitial air holes on Bragg gratings in photonic crystal fibres with a Ge-doped core by using the BPM. It is found that the interstitial air holes can make Bragg resonance wavelength λ_B shift a little towards short wavelength and increase the value of $\lambda_B - \lambda_1$, and coupling coefficient κ of Bragg resonance. Moreover, when the value of d/Λ is small, IAHs can suppress the cladding mode resonance. When the value of d/Λ is large, IAHs increase the number of modes that could strongly interact with the fundamental mode. The effect of interstitial air holes on transmission spectral characteristics of PCF-based FBG does not arise simply from the change in air-filling fraction. It is related to the distribution of interstitial air holes. The variability of λ_B is disadvantageous in fibre filter made of PCF-based FBG. The increase in coupling coefficient κ of Bragg resonance results in the broader full-width-at-half-maximum (FWHM) and the higher reflectivity of Bragg wavelength. The broad FWHM is disadvantageous in fibre filter made of PCF-based FBG, but the high reflectivity of Bragg wavelength is advantageous in fibre filter. And suppressing the cladding mode resonance is advantageous to high-quality filter.

References

[1] Knight J C, Birks T A, Russell P S J and Atkin D M 1996 *Opt. Lett.* **21** 1547

[2] Bjarklev A, Broeng J and Bjarklev A S 2003 *Photonic Crystal Fiber* (Boston: Kluwer Academic Publishers)

[3] Li S G, Liu X D and Hou L T 2003 *Acta Phys. Sin.* **52** 2811 (in Chinese)

[4] Eggleton B J, Westbrook P S, Windeler R S, Spalter S and Strasser T A 1999 *Opt. Lett.* **24** 1460

[5] Zhang C S, Kai G Y, Wang Z, Wang C, Sun T T, Zhang W G, Liu Y G, Liu J F, Yuan S Z and Dong X Y 2005 *Acta Phys. Sin.* **54** 2758 (in Chinese)

[6] Broeng J, Barkou S E, Bjarklev A, Knight J C, Birks T A and Russell P St J 1998 *Opt. Commun.* **156** 240

[7] Li Y F, Wang C Y, Hu M L, Liu B W, Sun X W and Chai L 2005 *Opt. Express.* **13** 6856

[8] Li S G, Li Y F, Zhang H J, Liu S Y, Zhou G Y, Han Y and Hou L T 2007 *Appl. Phys.* B **87** 71

[9] Yu X, Shum P, Tang M, Yan M and Love J 2006 *J. Optoelectronics and Advanced Materials* **8** 372

[10] Kim J C, Paek U C and Lee B H 2006 *Opt. Lett.* **31** 1196

[11] Eggleton B J, Westbrook P S, White C A, Kerbage C, Windeler R S and Burdge G L 2000 *J. Lightwave Tech.* **18** 1084

[12] Scarmozzino R, Gopinath A, Pregla R and Helfert S 2000 *IEEE J. Select. Topics Quantum Electron.* **6** 150

[13] She S X 2002 *The Physical Foundation of Waveguide Optics* (Beijing: Beijing Jiao Tong University Press) p387 (in Chinese)

[14] Erdogan T 1997 *J. Lightwave Technol.* **15** 1277

[15] Eggleton B J, Kerbage C, Westbrook P S, Windeler R S and Hale A 2001 *Opt. Express.* **9** 698

[16] Kerbage C, Eggleton B J, Westbrook P S and Windeler R S 2000 *Opt. Express.* **7** 113